The reactions were studied at constant temperature in a HETO 01 PT 623 thermostat.

Materials. Methanol used for preparation of reaction solutions was of spectroscopic quality, stored over 0.3-nm molecular sieves, otherwise of HPLC grade. *tert*-Butyl alcohol (p.a.) was purified by fractional recrystallization followed by drying over 0.4-nm molecular sieves. Pyridine (p.a.) was dried over KOH and then decanted and distilled from 0.4-nm molecular sieves; the center-cut was collected. Hexamethylenetetramine (Aldrich, Gold Label) was used without further purification. The purification of the other bases has been described previously.[14,20,25] All other chemicals were of reagent grade. Anhydrous sulfuric acid was used to buffer the reaction solutions (Table I and II).

Substrates. The syntheses of 9-(2-chloro-2-propyl)fluorene (**2**-Cl), the deuteriated analogue (9-^{2}H)-9-(2-chloro-2-propyl)fluorene (>99.0 atom % ^{2}H in the 9 position), and 9-(2-propenyl)fluorene (**5**) have been described recently.[24] The syntheses of 1-(2-chloro-2-propyl)indene (**1**-Cl),[11] 1-(2-bromo-2-propyl)indene (**1**-Br),[13] 9-(acetoxymethyl)fluorene (**3**-OAc),[13] and 9-(chloromethyl)fluorene (**3**-Cl)[25] have also been published.

Kinetics and Product Studies. The reaction vessel was a 2-mL HPLC flask sealed with a tight PTFE septum, placed in an aluminum block in the water thermostat, or, in the slower reactions and the reactions at higher temperature, consisted of 1-mL glass ampules. The reactions were initiated by rapid addition of the substrate dissolved in acetonitrile with a microsyringe to the prethermostated base solution in the HPLC flask or to a pear-shaped flask from which the mixed reaction solution was distributed to the glass ampules. The substrate concentration in the reaction solution was usually 0.05 mM in **2**-Cl or **3**-Cl and 0.12 mM in **1**-Cl. At appropriate intervals, samples (200 μL) of the reaction solution were transferred by means of a syringe (in the faster kinetic runs by means of a thermostated water-jacketed syringe) to an HPLC flask containing an appropriate amount of quench solution (prepared by diluting 15.6 mL of 2 M sulfuric acid with 40% ethanol–water to 250 mL) and analyzed. The mol % of the starting material and each of the products were measured, or, in some experiments, the starting material/internal-standard area ratio. The phenomenological rate constants were calculated from plots of ln (mol % starting material) or ln (area ratio) versus time and product data. Acenaphthene was used as internal standard in the kinetic experiments with **3**-Cl.

The samples from the kinetic runs with pyridine were quenched by shaking with a mixture of 700 μL of 1,1,1-trichloroethane, 10 mL of 2 M H_2SO_4, and 30 mL of water and ca. 10 g of ice in a 60-mL centrifuge tube. After centrifugation, the organic phase was washed by shaking with about 50 mL of cold water followed by a further centrifugation. The organic phase was then diluted with methanol and analyzed.

The kinetics of the reactions of **1**-Br were studied by UV spectrophotometry. The procedure has been described previously.[25]

Estimated errors are considered as maximum errors derived from maximum systematic errors and random errors.

Acknowledgment. The Swedish Natural Science Research Council and Ingegerd Bergh's Fund have financially supported this work. I also thank Professors Z. Rappoport, W. P. Jencks, R. A. More O'Ferrall, and D. J. McLennan for comments.

Registry No. **1**-Br, 75915-20-7; **1**-Cl, 64909-94-0; **2**-Cl, 56954-89-3; **3**-Cl, 36375-77-6; **3**-OAc, 63839-86-1; D_2, 7782-39-0.

Comparative Study of E2 and S_N2 Reactions between Ethyl Halide and Halide Ion

Tsutomu Minato[1a] and Shinichi Yamabe*[,1b]

Contribution from the Yuge Mercantile Marine College, Yuge-cho, Ochi-gun, Ehime 794-25, Japan, and Educational Technology Center, Nara University of Education, Takabatake-cho, Nara 630, Japan. *Received September 10, 1987. Revised Manuscript Received February 9, 1988*

Abstract: The transition-state (TS) geometries of bimolecular nucleophilic eliminations (E2) and substitutions (S_N2) between ethyl halides and halide ions are determined with ab initio MO calculations in order to probe the effect of the basicity of nucleophiles and the nucleofugality of the leaving groups on the reaction mechanism. E2 reactions dealt with here are found to the E2H category of the Bunnett's variable TS spectrum. The geometry of the E2 TS is shown to be entirely different from that of the S_N2 TS. Although the TS geometries of the syn and anti E2 reactions are calculated to be similar, their activation energies are different according to the extent of the intramolecular charge transfer.

The present paper describes a theoretical study on bimolecular nucleophilic reactions, especially eliminations (E2). There are many experimental studies of base-initiated alkene-forming β eliminations in the condensed phase.[2a-c] E2 reactions are also investigated in the gas phase to examine the intrinsic properties of the isolated systems.[2d-f] A recent study by Fourier transform ion cyclotron resonance mass spectroscopy has shown that the stability of the ion/molecule complex preceding the reaction barrier is important in determining the selectivity of the gas-phase E2.[2f]

E2 is the one-step process involving the simultaneous removal of the β-hydrogen and a leaving group and formation of a double bond. These bond interchanges need not be precisely synchronous.

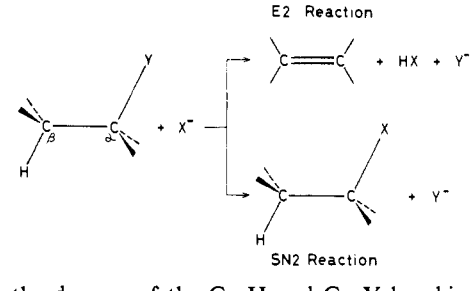

That is, the degrees of the C_β–H and C_α–Y breaking are not necessarily equal at the transition state (TS) of E2. Two theoretical models, Bunnett's variable E2H TS spectrum[3] and the Winstein–Parker E2C–E2H spectrum,[4] were put forth to deal with

(1) (a) Yuge Mercantile Marine College. Present address: Institute for Natural Science, Nara University, 1500 Misasagi-cho, Nara 631, Japan. (b) Nara University of Education.

(2) (a) Bartsch, R. A.; Zavada, J. *Chem. Rev.* **1980**, *80*, 453 and references cited therein. (b) McLennan, D. J. *Tetrahedron* **1975**, *31*, 2999. (c) Fry, A. *Chem. Soc. Rev.* **1972**, *1*, 163. (d) Doorn, R. V.; Jennings, K. R. *Org. Mass. Spectrom.* **1981**, *16*, 397. (e) DePuy, C. H.; Bierbaum, V. M. *J. Am. Chem. Soc.* **1981**, *103*, 5034. (f) Konig, L. J. d.; Nibbering, N. M. M. *J. Am. Chem. Soc.* **1987**, *109*, 1715.

(3) Bunnett, J. F. *Angew. Chem.* **1962**, *74*, 731.

(4) (a) Parker, A. J.; Winstein, S. *J. Am. Chem. Soc.* **1972**, *94*, 2240. (b) Parker, A. J. *CHEMTECH* **1971**, *1*, 297.

0002-7863/88/1510-4586$01.50/0

Chart I. Reactions and Numbers [1]–[30]

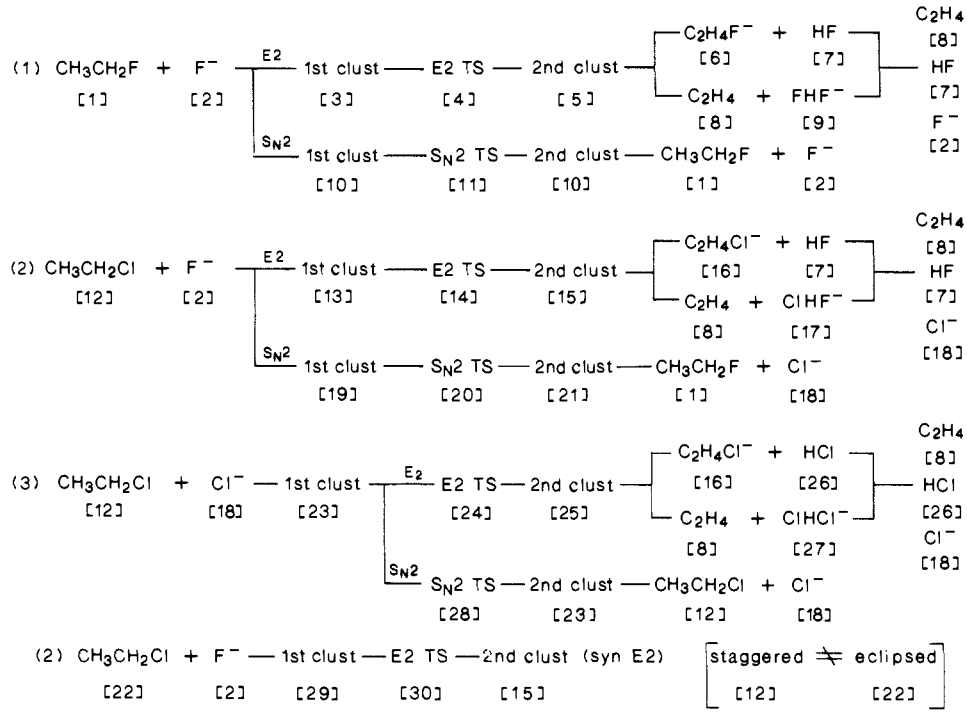

this concerted process flexibly. Both models are concerned with anti elimination.

Bunnett's model is characterized by the attack of X^- on the β-bonded hydrogen. β substitution by the electron-withdrawing group shifts the TS character to the right, but an electron donor at the C_α gives a leftward shift. An increase in the base strength leads also to a shift toward E2 and E1cB. In the Winstein–Parker

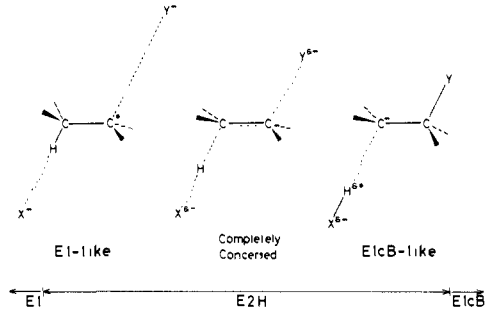

model, a partial $X^-\cdots C_\alpha$ loose covalent interaction is important (E2C and E2C-like). E2C pattern arises from the idea that a soft base, X^-, might have a common E2 and S_N2 TS.

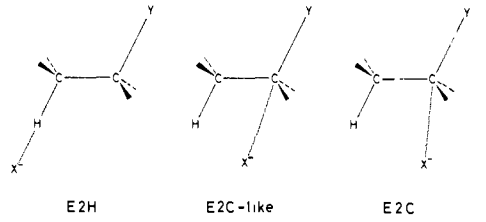

In these spectra, the position of the TS of a specific reaction is determined by the base strength of X^-, the nucleofugality[5] (ease of departure) of Y, and the substitution on the α and/or β site. The response of these mechanistic classes to kinetic, isotope, and leaving-group probes has been investigated extensively.

In this study, three nucleophilic eliminations and substitutions are analyzed by means of ab initio calculations. An explicit determination of the E2 TS structure and its electronic distributions is desirable. Three model reactions are investigated here: fluoroethane (EtF) with the fluoride ion (F^-) (1), chloroethane

$$F^- + EtF \rightarrow HF + CH_2{=}CH_2 + F^- \quad (1E)$$
$$\rightarrow EtF + F^- \quad (1S)$$
$$F^- + EtCl \rightarrow HF + CH_2{=}CH_2 + Cl^- \quad (2E)$$
$$\rightarrow EtF + Cl^- \quad (2S)$$
$$Cl^- + EtCl \rightarrow HCl + CH_2{=}CH_2 + Cl^- \quad (3E)$$
$$\rightarrow EtCl + Cl^- \quad (3S)$$

(EtCl) with F^- (2), and EtCl with the chloride ion (Cl^-) (3). Here, (1E) is the elimination and (1S) is the substitution of reaction 1. A comparison between reactions 1 and 2 may inform us of the reactivity–nucleofugality relation. The effect of the base strength is examined by a comparison between reactions 2 and 3. Our previous work on 1 revealed the structure of the first cluster, the TS, and the second cluster.[6] In the present work, the structure–reactivity variation is investigated. The first interest of this work is to assign TS geometries of our model systems to either E2H or E2C. The second interest lies in the stereoselectivity of the E2 reactions. That is, the TS structures of the anti and syn eliminations are compared in (2E), to determine if there is an intrinsic electronic difference of the reactivity in the two conformations.

For clarity, numbers [1]–[30] are attached to all the species involved in reactions 1–3 and are defined in Chart I.

Experimental Procedures

Calculations were carried out with the GAUSSIAN 80 program.[7] The 3-21G(+p) basis sets were used for the geometry optimization. For chlorine, carbon, and hydrogen atoms, the 3-21G basis set internal to the program was adopted. For a fluorine atom, a diffuse p-type GTO was added to the 3-21G basis set to describe the spread-out electron distribution of F^-, and its exponent is 0.074.[8a] The diffuse p orbital is not

(5) Stirling, C. J. M. *Acc. Chem. Res.* **1979**, *12*, 198.

(6) Minato, T.; Yamabe, S. *J. Am. Chem. Soc.* **1985**, *107*, 4621.

(7) GAUSSIAN 80: Binkley, J. S.; Whiteside, R. A.; Krishnan, R.; Seeger, R.; DeFrees, D. J.; Schlegel, H. B.; Topiol, S.; Kahn, L. R.; Pople, J. A. *QCPE* **1981**, *13*, *No. 406*. The program package of the vibrational analysis has been coded by Dr. K. Yamashita, to whom the authors are grateful.

Table I. Total Energies (Hartrees) of Four Methods on the 3-21G(+p) Optimized Geometries and the 3-21G Gibbs Free Energies ($G°$) in the Standard State (T 298.15 K, p 1 atm)[a]

no.	species	RHF/3-21G	MP2/3-21G	MP3/3-21G	RHF/DZP	$G°$
		Substrates, Reactants, and Products				
[1]	C_2H_5F	−177.133 41	−177.442 13	−177.455 23	−178.128 88	−177.085 61
[12]	C_2H_5Cl	−535.513 69	−535.743 60	−535.766 76	−538.138 17	−535.468 68
[22]	C_2H_5Cl (eclipsed)	−535.507 89	−535.737 60	−535.760 93	−538.131 62	−535.462 86
[2]	F^-	−98.915 47	−99.066 56	−99.050 04	−99.443 78	−98.929 63
[18]	Cl^-	−457.353 59	−457.396 89	−457.401 63	−459.503 81	−457.368 63
	(3-21G(+p))	(−457.376 74)				
	(3-21G*)	(−457.444 12)				
[8]	C_2H_4	−77.600 99	−77.780 11	−77.797 01	−78.050 38	−77.566 73
[7]	HF	−99.496 55	−99.631 46	−99.627 82	−100.049 17	−99.503 80
[26]	HCl	−457.869 43	−457.921 83	−457.929 04	−460.057 84	−457.880 80
[6]	$C_2H_4F^-$	−176.530 87	−176.860 14	−176.861 69	−177.507 61	−176.501 23
[9]	FHF^-	−198.493 07	−198.775 55	−198.757 88	−199.562 07	−198.502 41
[16]	$C_2H_4Cl^-$	−534.963 38	−535.186 77	−535.208 23	−537.564 33	−534.934 97
[17]	$ClHF^-$	−556.897 31	−557.079 76	−557.079 14	−559.597 65	−556.907 83
[27]	$ClHCl^-$	−915.265 94	−915.365 43	−915.375 60	−919.597 19	−915.283 90
		E2 Reaction of EtF with F^- (Figure 1, 1E)				
[3]	1st cluster	−276.075 25	−276.534 87	−276.532 22	−277.593 33	−276.030 53
[4]	TS	−276.029 50	−276.499 09	−276.492 26	−277.548 57	−275.989 87
[5]	2nd cluster	−276.051 07	−276.516 45	−276.513 74	−277.572 55	−276.013 33
		S_N2 Reaction of EtF with F^- (Figure 2, 1S)				
[10]	1st and 2nd clusters	−276.074 82	−276.533 54	−276.530 97	−277.594 37	−276.030 07
[11]	TS	−276.046 50	−276.510 80	−276.503 40	−277.556 70	−276.000 92
		E2 Reaction of EtCl with F^- (Figure 1, 2E; Figure 7)				
[13]	1st cluster	−634.458 44	−634.836 22	−634.844 26	−637.603 73	−634.417 63
[29]	1st cluster (eclipsed)	−634.437 33	−634.816 93	−634.825 08	−637.585 09	−634.395 42
[14]	TS (anti)	−634.443 41	−634.819 14	−634.827 56	−637.581 11	−634.407 82
[30]	TS (syn)	−634.420 52	−634.797 78	−634.806 41	−637.559 05	−634.384 86
[15]	2nd cluster	−634.479 55	−634.839 72	−634.856 63	−637.626 79	−634.442 84
		S_N2 Reaction of EtCl with F^- (Figure 2, 2S)				
[19]	1st cluster	−634.458 60	−634.833 82	−634.842 01	−637.604 78	−634.417 03
[20]	TS	−634.456 55	−634.827 11	−634.835 31	−637.596 20	−634.414 13
		(−634.477 37)[b]				
[21]	2nd cluster	−634.508 80	−634.862 38	−634.879 59	−637.652 49	−634.466 92
		E2 Reaction of EtCl with Cl^- (Figure 1, 3E)				
[23]	1st cluster	−992.891 28	−993.163 30	−993.191 06	−997.662 96	−992.851 96
[24]	TS	−992.832 62	−993.112 33	−993.137 24	−997.603 54	−992.800 91
[25]	2nd cluster	−992.846 67	−993.123 84	−993.151 84	−997.630 27	−992.815 17
		S_N2 Reaction of EtCl with Cl^- (Figure 2, 3S)				
[23]		1st and 2nd clusters, same as for the 1st cluster of 3E				
[28]	TS	−992.876 90	−993.145 36	−993.172 40	−997.639 74	−992.835 99
		(−993.058 37)[b]				

[a] To calculate the Gibbs free energy ($G°$) of substrate [22] and the first cluster [29] of the eclipsed form, an imaginary frequency corresponding to the rotation around the C–C bond is excluded. This is because they have unstable conformers. The first cluster of (1S), [10], the second cluster of (2E), [15], or the second cluster of (3E), [25], also have one imaginary frequency, which comes either from the error of the numerical differentiation of energy first derivative or from the invalidity of the harmonic approximation of the weak ion–dipole interaction. [b] In [20], the total energy (in parentheses) corresponds to the RHF/3-21G(+p+p′) optimized geometry of TS of (2S), where the chlorine p′ exponent is 0.0483. In [28] the total energy (in parentheses) corresponds to the RHF/3-21G* optimized geometry of the TS of (3S). These geometries are also given as supplementary material.

added to the chlorine 3-21G, because its inclusion leads to the overcorrection of the basis set superposition error (BSSE). For instance, the gas-phase binding energies of Cl^- and benzene are calculated to be 7.83 and 5.53 kcal/mol with the 3-21G and 3-21G(+p) (exponent = 0.055) basis sets, respectively. The experimental $\Delta H°$ is 9.9 kcal/mol.[13a] On the other hand, the absence of the diffuse p orbital on the fluorine atom leads obviously to the significant BSSE. For $F^-\cdots C_6H_6$, the binding energies are 38.66 kcal/mol with 3-21G and 13.02 kcal/mol with 3-21G(+p), while $\Delta H°_{exptl}$ is 15.3 kcal/mol.[8b]

The TS geometry was searched for by the gradient method implemented in the program. Determining the TS geometry in the E2 reaction is quite difficult, because the interchange of four chemical bonds occurs simultaneously. That difficulty has not been experienced in the search for the TS in various addition and substitution reactions. The delicate balance of the variables of the internal coordinates should be kept during the optimization.

Vibrational analyses on the stationary points were made. The Gibbs free energy $G°$ was calculated by the standard equation of statistical dynamics,[9] and the values are shown in Table I.

Total energies are recomputed with the second- and third-order Møller–Plesset perturbation scheme on the 3-21G(+p) geometries [MP2(3)/3-21G(+p)//RHF/3-21G(+p)]. Single-point calculations with the double-ζ plus polarization [RHF/DZP//RHF/3-21G(+p)] were made to examine the basis set dependence of the energy.[8c] These refined data are displayed in Tables I and II. All the geometries and their harmonic frequencies are given as supplementary material.

Results

Energy Diagram of E2 and S_N2 Reactions. Figure 1 shows the energy changes of the anti E2 reactions. All the E2 reactions are

(8) (a) Dunning, T. H., Jr.; Hay, P. J. *Modern Theor. Chem.* **1977**, *3*. Cf.: Clark, T.; Chandrasekhar, J.; Spitznagel, G. W.; Schleyer, P. v. R. *J. Comput. Chem.* **1983**, *4*, 294 and references cited therein. (b) Hiraoka, K.; Mizuse, S.; Yamabe, S. *J. Chem. Phys.* **1987**, *86*, 4102. (c) Huzinaga–Dunning DZ+p: Dunning, T. H. *J. Chem. Phys.* **1970**, *53*, 2823; *Ibid.* **1971**, *55*, 3958. On carbon, (9s5p1d) with the 1d exponent = 0.75; on fluorine, (9s5p1d1p) with the 1d exponent = 0.90 and 1p exponent = 0.074; on hydrogen, (4s1p) with the 1p exponent = 1.0; on chlorine, (12s8p1d) with the 1d exponent = 0.75.

(9) For instance: Knox, J. H. *Molecular Thermodynamics*; Wiley: New York, 1971.

Table II. Stabilizing Energies due to the Formation of the First Cluster (Ion–Dipole Complex) and TS Barrier Energies Relative to Energies of the First Clusters[a]

reaction	type	first cluster formation RHF/3-21G	MP2/3-21G	MP3/3-21G	RHF/DZP	TS energy barrier RHF/3-21G	MP2/3-21G	MP3/3-21G	RHF/DZP	figure showing RHF/DZP energy
F^- + EtF	1E	−16.5	−16.4	−16.9	−12.9	28.7	22.5	25.1	28.0	1 (1E)
	1S	−16.3	−15.6	−16.2	−13.6	17.8	14.2	17.3	23.6	2 (1S)
	2E	−18.4	−16.3	−17.3	−13.6	9.4	10.7	10.5	14.2	1 (2E)
F^- + EtCl	2E syn	−8.8	−8.0	−8.9	−6.1	10.6	12.0	11.7	16.3	7
	2S	−18.5	−14.8	−15.8	−14.3	1.3	4.2	4.2	5.4	2 (2S)
Cl^- + EtCl	3E	−15.1	−14.3	−14.2	−13.2	36.8	32.0	33.8	37.3	1 (3E)
	3S					9.0	11.2	11.7	14.6	2 (3S)

[a] All energies are calculated from those of Table I and are in kilocalories per mole.

composed of four elementary processes: formation of the first cluster (ion–dipole complex), E2 step, decomposition of the second cluster, and product formation. The stabilizing energies of the first-cluster formation of (1E) and (3E) are quite similar (−13.0 vs −13.2 kcal/mol). After the E2 step, the second cluster is produced. It decomposes further either into $CH_2{=}CH_2{\cdots}Y^-$ and HX or into $CH_2{=}CH_2$ and $(XHY)^-$. The latter process is more favorable in three cases. In (1E), (2E), and (3E), only one energy maximum is obtained in the E2 step. That is, no energy minimums are found during the bond interchange. This result demonstrates that (1E), (2E), and (3E) are concerted processes.

Figure 2 shows the energy profiles of three S_N2 reactions. All the S_N2 reactions have three elementary processes: formation of the first cluster, the S_N2 step, and the decomposition of the second cluster. The stabilizing energies of the first-cluster formation of (1S) and (2S) are almost the same as the corresponding energies of the E2 reactions in Figure 1. It is noted that the energy level of the S_N2 first cluster in (3S) is the same as that of the E2 first cluster in (3E). That is, only one first-cluster structure is obtained in the system of EtCl and Cl^-. This is discussed below. As with the E2 results, (2S) is the most facile reaction among the three. It is noteworthy that the energy barrier of (1S) (23.6 kcal/mol) is larger than that of (3S) (14.6 kcal/mol), while the comparison of the E2 barriers in Figure 1 gives the opposite result [28.1 for (1E) vs 37.3 kcal/mol for (3E)]. The principle of hard and soft acids and bases[10] is applicable to this contrast. The hard nucleophile F^- prefers the hard site C_β–H, while the soft anion Cl^- attacks favorably the soft reactive site C_α. In fact, only the E2 reaction of EtF and F^- is possible in the gas phase,[11] while the S_N2 reaction occurs exclusively in the gas phase between bromoethane and Cl^-.[12]

The effect of the electron correlation and the basis set dependence on the potential energy are examined in Table II. Both the first-cluster stabilizing energies and the TS barrier energies are more sensitive to the basis set (3-21G vs DZP) than to the correlation correction. The double-ζ plus polarization (DZP) decreases the former energies and enlarges the latter ones. The origin of these changes may be the difference of the calculated dipole moments (μ's, in debye). For the substrate EtF, μ(3-21G(+p)) = 2.97 D, μ(DZP) = 2.59 D, and μ(exptl) = 1.96 D. The significantly overestimated μ's with the 3-21G(+p) leads to the overstabilization energy of the first cluster (ion–dipole complex) and to the too small activation energy. Thus, the decrease of the calculated polarity of all the species seems to correspond to the improvement of the energies.

The first-cluster stabilizing energies may be compared to the chloride and fluoride ion affinities estimated through the measurement of the ion cyclotron resonance by Larson and McMahon.[13] The chloride binding energy in $Cl^-{\cdots}CH_3Cl$ was reported

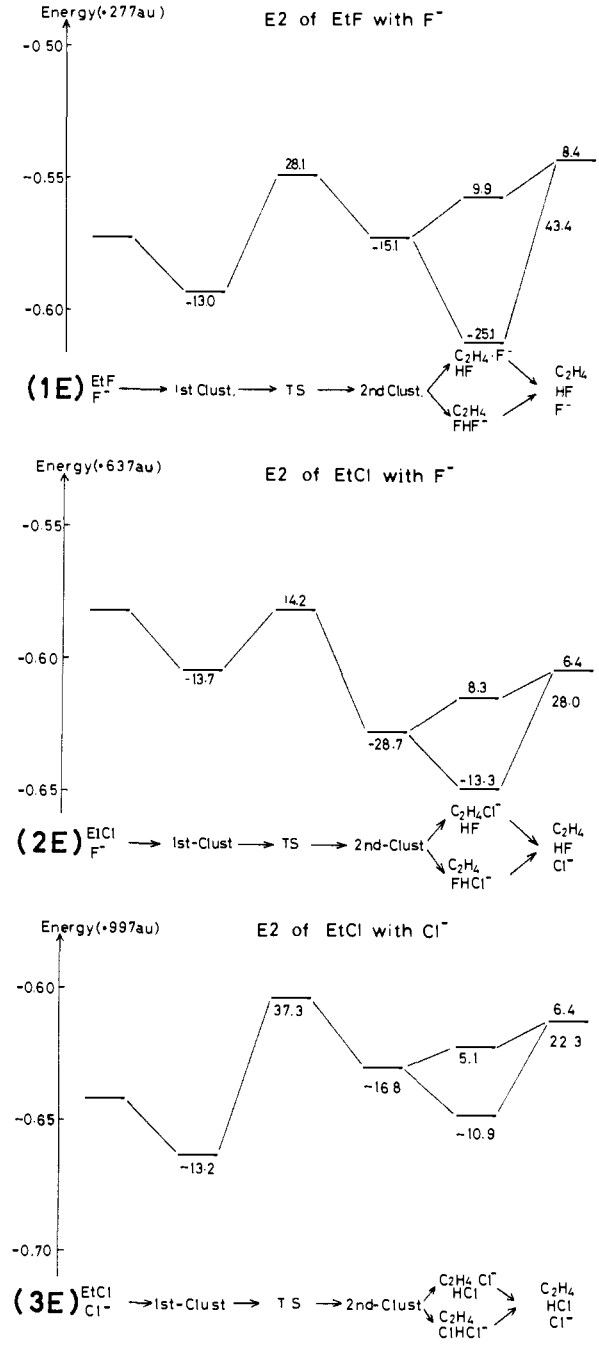

Figure 1. Energy diagrams of three E2 reactions with the double-ζ plus polarization basis set (RHF/DZP//RHF/3-21G). Values attached to energy levels are in kilocalories per mole and show the stabilization (<0) and the destabilization (>0) relative to the left adjacent levels. Clust denotes the cluster (ion–dipole complex). TS stands for the transition state. (1E) E2 of EtF and F^-; (2E) E2 of EtCl and F^-; (3E) E2 of EtCl and Cl^-.

(10) Pearson, R. G. *J. Chem. Educ.* **1968**, *45*, 581.
(11) (a) Ridge, D. P.; Beauchamp, J. L. *J. Am. Chem. Soc.* **1974**, *96*, 637; *Ibid.* **1974**, *96*, 3595. (b) Sullivan, S. A.; Beauchamp, J. L. *Ibid.* **1976**, *98*, 1160.
(12) Caldwell, G.; Magnera, T. F.; Kebarle, P. *J. Am. Chem. Soc.* **1984**, *106*, 959.
(13) (a) Larson, J. W.; McMahon, T. B. *J. Am. Chem. Soc.* **1984**, *106*, 517. (b) Larson, J. W.; MacMahon, T. B. *Ibid.* **1985**, *107*, 766.

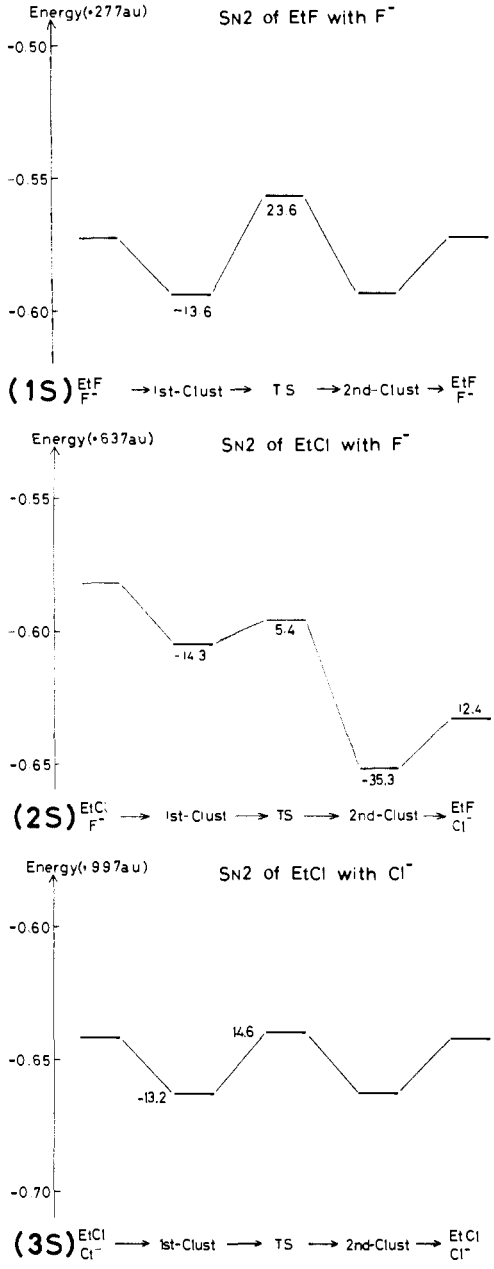

Figure 2. Energy diagrams of three S_N2 reactions. Same notations as in Figure 1 are used. (1S) S_N2 of EtF and F^-; (2S) S_N2 of EtCl and F^-; (3S) S_N2 of EtCl and Cl^-.

to be 12.2 kcal/mol. This value is in good agreement with the DZP energy of (3E) and (3S) but is somewhat smaller than the MP3 energy, 14.3 kcal/mol. Although the experimental fluoride ion affinity pertinent to our first-cluster system is not available in the literature, our DZP F^-···EtF and F^-···EtCl energies (~14 kcal/mol) are probably smaller than the real ones, and the MP3 energies would be better. However, the overall profile of the potential energy is not dependent so much on the accuracy of the wave function.

Structures of the E2 and S_N2 First Clusters. Figure 3 gives the geometries of two substrates and three anti E2 first clusters. Their analyses may be informative to the gas-phase E2 experiment. The positional difference between the reagents F^- and Cl^- is noticeable in the cluster. In (1E) and (2E), F^- with a small ion radius (1.36 Å) is bonded to the β-hydrogen moderately. On the other hand, Cl^- with the larger ion radius (1.81 Å) is located at the backside of the C_α–Cl bond in (3E). For (3E), there is only one first cluster common to the E2 and S_N2 reactions. To predict the reaction path from the first cluster, the in-plane vibrational mode of a low-frequency stretching is examined. Naturally, this mode indicates the approach of X^- toward the C_β–H bond of the substrate.

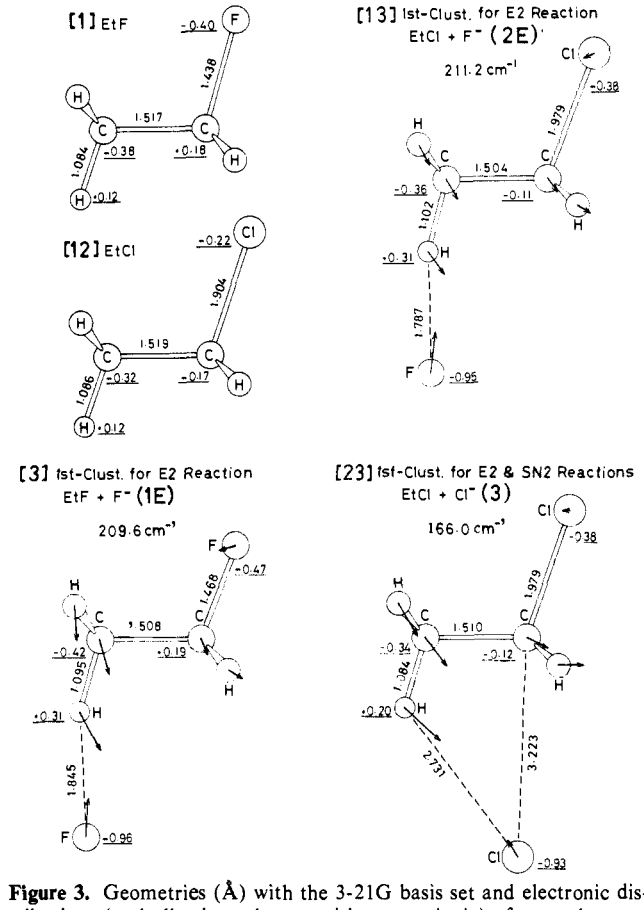

Figure 3. Geometries (Å) with the 3-21G basis set and electronic distributions (underlined numbers, positive → cationic) of two substrates and three E2 first clusters with the DZP basis set. For clusters, the normal vibration mode of the lowest frequency in the plane is drawn together with its frequency (cm^{-1}). The numbers [1], [12], [3], etc., are defined in Chart I, and all the geometries are given by the Cartesian coordinates in the supplementary material.

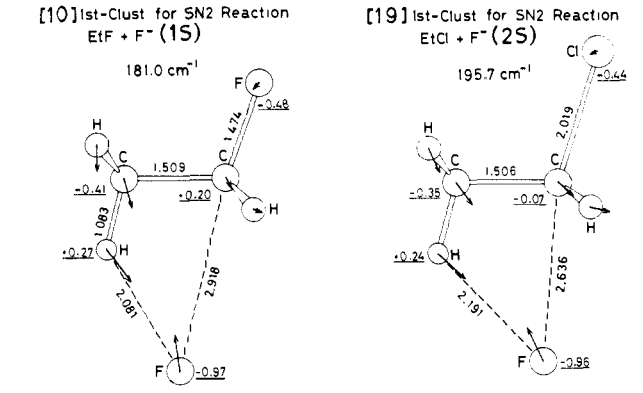

Figure 4. Geometries (3-21G) and electronic distributions (DZP) of two S_N2 first clusters. The same notations as in Figure 3 are used. The S_N2 cluster of (3S) is omitted, because it is common to the E2 cluster shown in Figure 3.

Figure 4 shows the S_N2 first clusters. F^- is located at the backside of C_α–Y. However, the stretching mode of the low frequency indicates the trend that F^- attacks the C_β–H bond rather than the C_α for the Walden inversion. Acidic β-hydrogens are better targets for F^-. Two kinds (E2 and S_N2) of first clusters in (1) and (2) are transferable with each other [small energy barrier for the F^- migration, e.g., less than 0.5 kcal/mol for (1)]. The E2 and S_N2 clusters are nondistinguishable in the thermal condition.

Transition-State Geometries of E2 and S_N2. Figure 5 shows three anti E2 transition states. Bond distances are given together with their elongation ratios by percent.[14] Although Figure 1

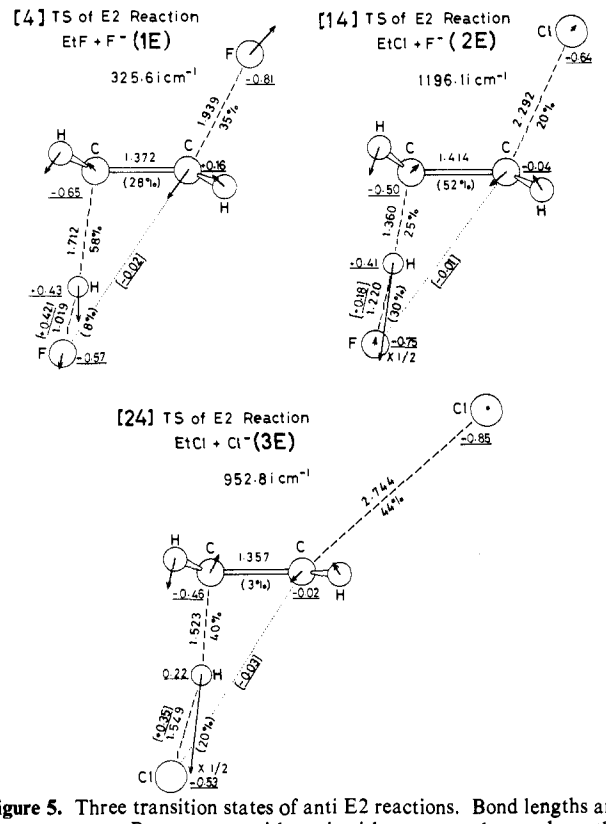

Figure 5. Three transition states of anti E2 reactions. Bond lengths are in angstroms. Percentages with and without parentheses show the elongation ratio of bonds to those of substrates or products. Underlined numbers denote net charge distributions with DZP, and those in brackets are $X^-\cdots H_\beta$ and $X^-\cdots C_\alpha$ atom–atom bond populations (positive, bonding). Vibration modes indicating the reaction paths are also exhibited together with their sole imaginary frequencies. On the leaving β-hydrogen of (2E) and (3E), the half-size of the displacement vectors is sketched ($\times^1/_2$).

indicates that (1E), (2E), and (3E) are all concerted eliminations, their TS structures are appreciably different. In view of the percentages, the extent of the bond formation and cleavage may be tabulated in the following order: X–H bond formation, (1E) > (3E) > (2E); C_β–H bond cleavage, (1E) > (3E) > (2E); double bond formation, (3E) > (1E) > (2E); C_α–Y bond cleavage, (3E) > (1E) > (2E). In the above comparison, the bond interchange in (2E) is the most incomplete. In other words, (2E) is of the earliest TS's among the three. It is natural that the strong nucleophile F^-[15] and the readily leaving group Cl^- give this character. The bond interchange in (1E) is advanced at the β site, while that in (3E) is around C_α. The character of these TS's may be analyzed more clearly by the vibration mode indicating the reaction path. These modes correspond to the sole imaginary frequencies, of which the absolute values show the sharpness of the potential energy surface near TS along the reaction coordinate. The "early" TS of (2E) has the largest absolute value. The major component of the vibrational mode is located at the C_β–H bond cleavage, followed by the growth of the ethylenic planarity. The vibrational mode of (3E) is also of the C_β–H bond cleavage. The leaving group Cl^- has already departed. On the other hand, the major vibrational mode of (1E) is the C–F bond stretching. At the TS, the C_β–H bond is almost broken. Although three TS's have somewhat different natures, they are all E2H types. No compromise-type TS's between E2 and S_N2 (i.e., E2C) are obtained.

Three S_N2 TS structures are depicted in Figure 6. To avoid the steric repulsion by the methyl group $C_\alpha H_3$, the $Y\cdots C_\alpha\cdots X^-$ is

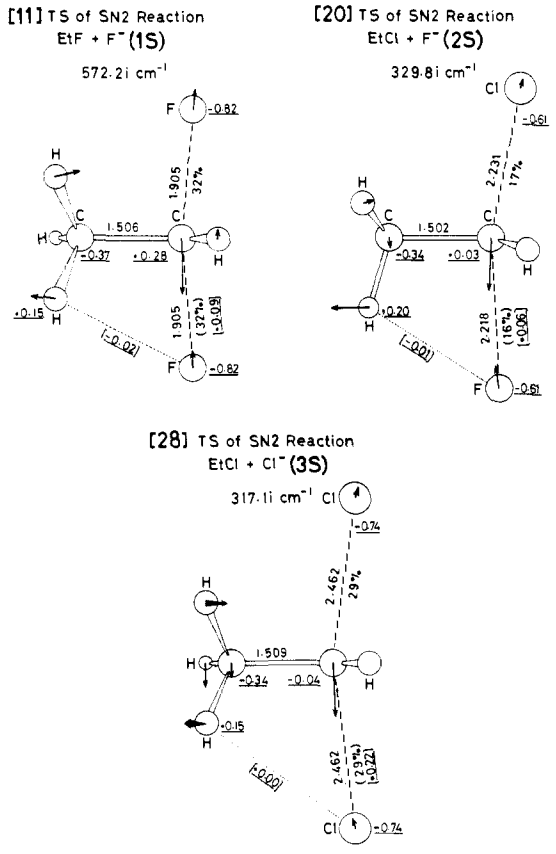

Figure 6. Three transition states of S_N2 reactions. The same notations as in Figure 5 are used.

slightly bent in three TS's. Thus, the S_N2 TS is entirely different from the E2 TS. Like the E2 TS, the S_N2 TS of (2S) is early in view of the small percentage (17%).

In Figures 5 and 6, the $X^-\cdots H_\beta$ and $X^-\cdots C_\alpha$ atom–atom bond populations are exhibited in brackets. They may be criteria for distinguishing E2H from E2C. That is, if both populations show the bonding nature in a TS, it is of the E2C type. In Figure 5, all $X^-\cdots C_\alpha$ densities are antibonding. In Figure 6, no $X^-\cdots H_\beta$ bonding components are found. Thus, our TS geometries are found to be E2H type in the electronic distribution.

Two types of basis set dependence of the TS geometry are examined. First, the effect of the presence or the absence of the chlorine diffuse p orbital (p′) on the TS geometry of S_N2 (2S) is examined. Without it, the newly formed C···F bond length is 2.218 Å and the C···Cl length to be broken is 2.231 Å (in Figure 6). With it (exponent = 0.0483), they are 2.342 and 2.161 Å, respectively. About 0.1-Å difference is found in both C···F and C···Cl lengths, which is not so significant as to affect our discussion. Second, the basis set dependence of the TS geometry is examined in (3S). The C···Cl length is 2.462 Å (3-21G) or 2.452 Å (3-21G*). The angle Me–C–Cl is 97.98° (3-21G) or 98.15° (3-21G*). This result indicates that the TS structure is rather insensitive to the choice of the basis set. The stabilizing energies by 3-21G(+p) → 3-21G(+p+p′) are 14.5 kcal/mol for Cl^- and 13.1 kcal/mol for the TS of (2S), respectively (see the RHF/3-21G energies in parentheses in Table I). Those by 3-21G → 3-21G* are 56.8 kcal/mol for Cl^- and 113.9 (≅56.8 × 2) kcal/mol for the TS of (3S), respectively. That is, the lowering energy of the chloride ion by the polarization function is almost the same as that of the TS. Such a parallel energy shift demonstrates that the polarization function on the chloride ion is not so important in seeking the potential energy surface.

Comparison of TS's between Anti and Syn E2 Reactions. The factors that determine whether anti or syn elimination predominates are examined. Figure 7 shows the energetics of anti and syn E2 reactions for (2E). The energy difference of staggered and eclipsed substrates (DZP) is 4.1 kcal/mol, and that of anti and syn TS's is 13.8 kcal/mol. The anti E2 proceeds more readily

(14) For instance in (1E), 58% of the C_β–H bond is obtained by (1.712 − 1.084)/1.084 × 100 and 28% of the C_α–C_β bond is (1.372 − 1.315)/0.202 × 100, where 1.315 is the ethylenic C=C distance and 0.202 is the difference between the C=C bond and the C—C bond in EtF.

(15) In the gas phase, the basicity coincides with the nucleophilicity. Therefore, in this text, F^- is a more nucleophilic base than Cl^-. This is not true for the nucleophilic reactions in protic solvents.

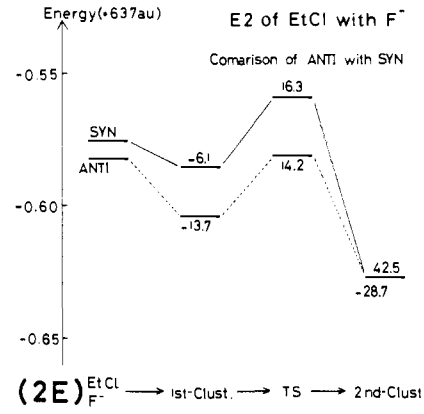

Figure 7. Energy diagrams of anti and syn E2 reactions.

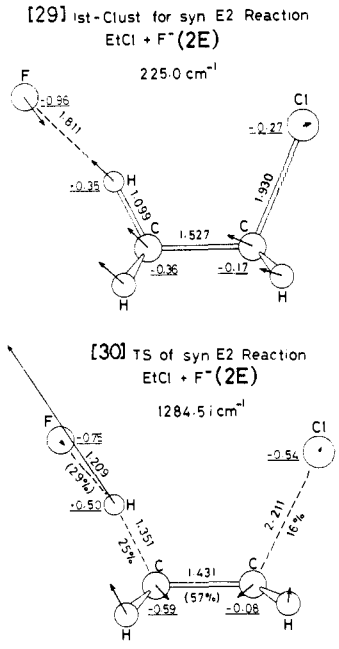

Figure 8. Geometries of the first cluster and the transition state of syn E2 of EtCl and F^-. The same notations as in Figure 5 are used.

through the smaller activation energy.

Figure 8 presents the geometries of the first cluster and the TS of the syn E2 reaction. In the first cluster, an imaginary vibration frequency is obtained, and it shows a rotational mode around the C_α–C_β bond (not shown). The instability of the eclipsed conformer is the source of the frequency. In the TS, interestingly, the rotational mode does not give an imaginary frequency. This result indicates that the TS geometry in Figure 8 corresponds to the energy minimum with respect to the rotation. The switch of the energy maximum at the first cluster to the minimum at the TS is ascribed to the formation of the C_α–C_β π bond. The semi-π bond (1.431 Å) of the TS has enough power to fix the unstable eclipsed form. Therefore, the TS of the syn E2 reaction is also the real TS. The first cluster and TS of the syn E2 reaction are similar in geometry to those of the anti E2 reaction, respectively. The small difference in the bond distances reflects that between the staggered and eclipsed forms of EtCl. The nonlinearity of the F^-···H–C_β in the syn E2 reaction arises from the F^-···Cl steric (ionic) repulsion. Thus, for the simple substrate, the TS's of anti and syn eliminations are found to be of geometric similarity.

Discussion

Anti E2 vs S_N2. E2 reactions 1E, 2E, and 3E are concerted and belong to the E2H category. It is understandable that they are not in the E1cB region outside the E2H, because two substrates, EtF and EtCl, have no substituents. Schleyer et al. reported that the E1cB intermediate 2-fluoroethyl anion is absent.[16] Electron-withdrawing substituents and/or a leaving group with lower nucleofugality may lead to the E1cB mechanism. Thus, our simple substrates react in the E2H category. However, the E2 TS becomes more carbanionic (more E1cB-like) by the combination of a strong base and a poor leaving group; (1E) affords an example. A comparison of (2E) with (3E) shows the effect of the base strength ($F^- > Cl^-$ in the gas phase) on the TS structure in Figure 5. With a stronger base, less C_α–Cl bond breaking is found. This is in agreement with the experimental results.[17]

Neither E2C-like nor E2C TS is found in our E2 reactions. On the contrary, X^- bonded to the H_β has escaped slightly from the backside region of the C_α–Y bond (X^-···H···C_β, nonlinear). That is, the attacking base X^- does not approach the C_α at the TS. This result is reasonable in consideration of the π-bond formation between C_α and C_β. The π-bond formation expels an attacking base from the C_α–C_β region to avoid the exchange repulsion. This

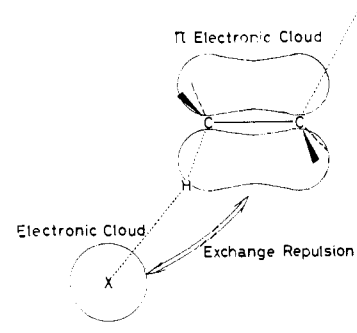

tendency is clearly shown in the comparison of Figure 5 with Figure 6. In the S_N2 TS (no π bond) of Figure 6, the line of the Y–C_α almost makes a right angle against the C_α–C_β bond. On the other hand, Figure 5 shows that the leaving group F (or Cl) goes away from the C–C region as the π bond is formed. Thus, the E2C TS geometry is not found here, because the base X^- is engrossed in the completion of the X–H_β bond avoiding the exchange repulsion.

Anti E2 vs Syn E2. The stereoselectivity of the E2 reactions is discussed in Figures 7 and 8. In general, the superiority of the anti E2 reaction is explained on two grounds. The first is concerned with the stability of the substrates. The substrate of the staggered form is of lower energy than that of the eclipsed one, particularly with bulky substituents on C_α or C_β. The second is concerned with the activation energy difference, i.e., the difference in the extent of the intramolecular charge transfer (CT) in the sense of the E1cB mechanism. Which ground is more important

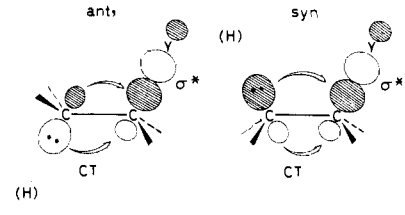

to explain the superiority of anti? The energy gap of staggered and eclipsed substrates is smaller than the difference of the height of the TS energies in Figure 7. This result indicates that the second explanation is more important for determination of syn/anti selectivity. The intramolecular CT in anti is more effective in pushing out the leaving group Y from the backside direction (like S_N2).

Bach et al. pointed out that the syn E2 reaction has an E1cB mechanism.[18] That is, the expulsion of the leaving group occurs concomitantly with the inversion of the configuration at C_β. The need for rehybridization at C_β makes the syn mechanism unfavorable. However, the motion leading to the inversion of the

(16) Schleyer, P. v. R.; Kos, A. J. *Tetrahedron* **1983**, *39*, 1141.
(17) Baciocchi, E. *Acc. Chem. Res.* **1979**, *12*, 430.
(18) Bach, R. D.; Badger, R. C.; Lang, T. J. *J. Am. Chem. Soc.* **1979**, *101*, 2845.

configuration at C_β is not found at the syn TS. Probably, the minimum energy path sought by Bach et al.[18] deviates significantly from the true reaction coordinate.

Solvent Effect on E2 and S_N2. In the condensed phase, the β-hydrogen atom (acidic, shown in Figure 3) and the nucleophile X^- are surrounded by solvent molecules. Therefore, in the protic solvent, the first cluster is not formed, and the base strength is weakened considerably. The double desolvation (at the β proton and X^-) is required to arrive at the E2 TS, whereas the single desolvation (at X^-) is needed for S_N2. Thus, S_N2 proceeds more readily than E2 in the polar solvent. The most reactive site, H_β, in the gas phase is the most strongly solvated site to block the X^- attack.

Although the energy profile in the gas phase in Figures 1 and 2 is entirely different from that in the condensed phase, TS geometries are common to both phases. The solvation strength is essentially electrostatic, which cannot alter the geometric configuration. The invariance of the geometry with and without solvent molecules has been found in several studies. Bertrán et al. searched for the first-cluster and TS geometries of S_N2 reactions: $F^- + CH_3F \rightarrow FCH_3 + F^-$ (gas phase) and $(H_2O)F^- + CH_3F(H_2O) \rightarrow (H_2O)FCH_3 + F^-(H_2O)$.[19] At the first cluster, the F···C distances are 2.31 and 2.33 Å without and with two water molecules, respectively. At TS, they are 1.78 and 1.79 Å. The invariance of the distance without and with solvent (water) molecules is surprising in view of the large $F^-\cdots H_2O$ binding energy (=23.3 kcal/mol, experimental).[13b] This result demonstrates that the solvation strength is mainly electrostatic.

In addition, recent theoretical studies have shown that the activation energies in the gas phase and aqueous media may be qualitatively reproduced in an S_N2 reaction: $Cl^- + CH_3Cl \rightarrow ClCH_3 + Cl^-$.[20] The solvation by over 200 water molecules is taken into account in the Monte Carlo simulation. Each water molecule is represented by four point charges ("TIP4P model"). The model prohibits the $Cl^- \rightarrow H_2O$ charge transfer and other (exchange and polarization) interactions. The validity of the model of the hydrated S_N2 reaction indicates again that the solvation may be described well as the Coulombic stabilization. In view of these results, our TS geometries may be applicable to the condensed-media reactions.

Concluding Remarks

The determination of the TS structures of three E2 and S_N2 reactions gives some information. All the eliminations are concerted and belong to the E2H category of Bunnett's variable TS spectrum. The elimination of EtCl by F^- has an early TS, while that of EtCl by Cl^- is late. The E2 TS is completely different from the S_N2 TS in three reactions adopted here, because the incipient π-electronic cloud expels an attacking base from the C_α–C_β region in the E2 TS.

The geometry of the syn E2 TS is similar to that of the anti TS. But, the syn – anti activation energy difference is larger than the conformational energy gap of eclipsed and staggered substrates. The extent of the intramolecular CT is the source of the former difference.

Acknowledgment. We thank the Institute for Molecular Science for the allotment of the CPU time of the HITAC M-680H computer.

Registry No. EtF, 353-36-6; EtCl, 75-00-3; F^-, 16984-48-8; Cl^-, 16887-00-6.

Supplementary Material Available: Tables of Cartesian coordinates and vibrational frequencies (16 pages). Ordering information is given on any current masthead page.

(19) Jaume, J.; Lluch, J. M.; Oliva, A.; Bertrán, J. *Chem. Phys. Lett.* **1984**, *106*, 232.

(20) (a) Chandrasekhar, J.; Smith, S. F.; Jorgensen, W. L. *J. Am. Chem. Soc.* **1985**, *107*, 154. (b) Chandrasekhar, J.; Jorgensen, W. L. *Ibid.* **1985**, *107*, 2974.

Chiroptical Properties of Chiral Olefins[1]

Aharon Gedanken,*,† M. Duraisamy,‡ Jiling Huang,‡ J. Rachon,‡,[2] and H. M. Walborsky*,‡

Contribution from the Department of Chemistry, Bar-Ilan University, Ramat-Gan, Israel 52100, and the Department of Chemistry, Florida State University, Tallahassee, Florida 32306-3006.
Received November 2, 1987

Abstract: A series of chiral (4-methylcyclohexylidene)(X,Y-substituted)methane derivatives have been prepared (i.e. X = CH_3, H, D and Y = Cl, Br, F). Their CD spectra in the vacuum ultraviolet have been recorded and discussed.

The optical activity of the olefin chromophore has been the subject of extensive theoretical[3-6] and experimental[7-15] investigation. The most comprehensive study of chiral olefins was undertaken by Drake and Mason.[3] They successfully assigned the first transition of the olefinic chromophore as the $\pi \rightarrow$ 3s Rydberg by dissolving the chiral olefin in a variety of solvents whereby the $\pi \rightarrow$ 3s broadened appreciably and was shifted to higher frequencies. When the solution was cooled, the Rydberg excitation continued to shift to higher energies. A different behavior was observed for the $\pi \rightarrow \pi^*$, which was shifted in solution to lower energies. The circular dichroism (CD) of the symmetric olefin, whose optical activity is due to dissymmetrically located substituents, originates from the coupling between the electric dipole allowed $\pi \rightarrow \pi^*$ transition and the magnetic dipole allowed $\pi \rightarrow$

† Bar-Ilan University.
‡ Florida State University.

(1) Partial support of this work by a grant from the National Science Foundation to one of us (H.M.W.) is gratefully acknowledged.
(2) Visiting Professor from the Institute of Organic Chemistry, Technical University, Gdansk, Poland.
(3) Drake, A. F.; Mason, S. F. *Tetrahedron* **1977**, *33*, 937.
(4) Weigang, O. E. *J. Am. Chem. Soc.* **1979**, *101*, 1965.
(5) Liskow, D. H.; Segal, G. A. *J. Am. Chem. Soc.* **1978**, *100*, 2945.
(6) Yaris, M.; Moscowitz, A.; Berry, R. S. *J. Phys. Chem.* **1968**, *49*, 3150.
(7) Paquette, L. A.; Kearney, F. R.; Drake, A. F.; Mason, S. F. *J. Am. Chem. Soc.* **1981**, *103*, 5064.
(8) Paquette, L. A.; Doecke, C. W.; Kearney, F. R.; Drake, A. F.; Mason, S. F. *J. Am. Chem. Soc.* **1980**, *102*, 7229.
(9) Mason, M. G.; Schnepp, O. **1973**, *59*, 1092.
(10) Gross, K. P.; Schnepp, O. *Chem. Phys. Lett.* **1975**, *36*, 531.

0002-7863/88/1510-4593$01.50/0